

# The Mass Distribution of Population III Stars

M. Fraser<sup>1\*</sup>, A. R. Casey<sup>1</sup>, G. Gilmore<sup>1</sup>, A. Heger<sup>2,3,4</sup>, C. Chan<sup>2</sup>

<sup>1</sup>*Institute of Astronomy, University of Cambridge, Madingley Road, Cambridge CB3 0HA, UK*

<sup>2</sup>*Monash Centre for Astrophysics, School of Physics and Astronomy, Monash University, 19 Rainforest Walk, Vic 3800, Australia*

<sup>3</sup>*Department of Physics and Astronomy, Shanghai Jiao-Tong University, CNA, Shanghai 200240, P. R. China*

<sup>4</sup>*School of Physics and Astronomy, University of Minnesota, Minneapolis, MN 55455, USA*

Accepted 2015 XX XX. Received 2015 November XX; in original form 2015 November xx

## ABSTRACT

Extremely metal-poor stars are uniquely informative on the nature of massive Population III stars. Modulo a few elements that vary with stellar evolution, the present-day photospheric abundances observed in extremely metal-poor stars are representative of their natal gas cloud composition. For this reason, the chemistry of extremely metal-poor stars closely reflects the nucleosynthetic yields of supernovae from massive Population III stars. Here we collate detailed abundances of 53 extremely metal-poor stars from the literature and infer the masses of their Population III progenitors. We fit simple initial mass function to the ensemble of inferred Population III star masses, and find that the mass distribution is well-represented by a power law IMF with exponent  $\alpha = 2.35^{+0.29}_{-0.24}$ . The inferred maximum progenitor mass for supernovae from massive Population III stars is  $M_{\max} = 87^{+13}_{-33} M_{\odot}$ , and we find no evidence for a contribution from stars with masses above  $\sim 120 M_{\odot}$ . The minimum mass is strongly consistent with the theoretical lower mass limit for Population III supernovae. We conclude that the IMF for massive Population III stars is consistent with the initial mass function of present-day massive stars and there may well have formed stars much below the supernova mass limit that could have survived to the present day.

**Key words:** stars, stars: abundances, stars: formation

## 1 INTRODUCTION

Population III stars formed from primordial metal-free gas, and can be subdivided into Population III.1 and III.2 stars. The former are completely unaffected by preceding star formation, while the latter may have been effected by energy input from previous star formation, but not chemically enriched (O’Shea et al. 2008). Of these stars, only those which had masses below  $\lesssim 0.8 M_{\odot}$  could have survived to the present day. No low mass Population III star has been discovered thus far, however, despite decades of intensive searching (e.g., Beers & Christlieb 2005; Christlieb et al. 2008; Norris et al. 2013; Jacobson et al. 2015; Schlafman & Casey 2014). The absence of an unambiguous detection of a low mass Population III star means that both the individual and ensemble properties of these stars remains unknown. The initial mass function (IMF) which governs the relative frequency of stars as a function of mass, appears to be fairly uniform today (Bastian et al. 2010). In the early universe, however, the conditions for star formation were presumably quite different, and there have long been theoretical argu-

ments that many more extremely massive ( $\sim 10^2 - 10^3 M_{\odot}$ ) stars would have formed (e.g., Bromm et al. 1999). More recently, this has been questioned, with increased spatial resolution in simulations of metal-free star formation and an improved understanding of the role of cooling from molecular hydrogen. This work suggests that fragmentation occurs, and that lower-mass metal-free stars can be produced (e.g. Clark et al. 2011; Greif et al. 2011).

To determine the IMF for Population III stars, we need to count the number of massive stars in the early Universe. Because we cannot observe individual members of the first generation of massive stars in the foreseeable future, we are forced to turn to indirect tracers. One such probe is spectroscopy of galaxies, which can reveal the signature of a large number of Population III stars (Schaerer 2002; Sobral et al. 2015). Alternatively, one can search for the explosion of Population III stars as high redshift supernovae (Whalen et al. 2013). Finally, it is also possible to study Population III stars through their chemical imprint on subsequent generations of low mass stars (Heger & Woosley 2002, 2010).

Extremely metal-poor (EMP) stars are thought to have formed out of material that has been enriched by very few (or just one) supernovae. Because the photospheric abun-

\* E-mails: mf,arc,gil@ast.cam.ac.uk

dances remain largely unchanged throughout a star's lifetime, the abundances measured in EMP stars from high-resolution spectra reflect the composition of the gas from which that star formed. If this gas has been polluted by only a single supernova, then these same abundances provide information on its progenitor and explosion parameters. Through comparison to models of supernova nucleosynthesis, we can infer both the mass of the progenitor and the supernova explosion energy (Tominaga et al. 2014; Placco et al. 2015; Ji et al. 2015).

In this Letter we assemble a large sample of EMP stars from the literature, and use them to determine the mass range of massive Population III stars and infer the slope of the IMF. We also consider whether there is any evidence for pair instability supernovae based on the chemical abundances of stars in the Milky Way. In Sections 2 and 3 we outline our literature sample of observational data, the methodology for determining the mass of the progenitors of Population III SNe, and the procedure for fitting the IMF. In Section 4 we discuss our results and draw conclusions.

## 2 DATA

We searched the literature for EMP stars with detailed chemical abundances. For stars with progressively higher metallicities, there is a greater likelihood that the star has been polluted by multiple generations of previous supernovae. Indeed, given the right combination of progenitor mass and explosion energy, a single primordial supernova can enrich some of the interstellar medium to a level of  $[\text{Fe}/\text{H}] \sim -3$  (e.g., Chen et al. 2015). For these reasons we place an arbitrary cut of  $[\text{Fe}/\text{H}] < -3.5$  on our sample. This threshold provides us with a sufficient number of metal-poor stars with detailed chemical information ( $\sim 50$ ), but limits the number of stars that are more likely to have formed from multiple supernovae.

We first queried the **SAGA** database<sup>1</sup> for all stars with metallicities  $[\text{Fe}/\text{H}] < -3.5$ . We complemented this search with recently published works from the literature. For stars with chemical abundances published in multiple papers, we tended towards more recent literature sources which included large samples of metal-poor stars. We sourced measured abundances directly from the original literature (i.e., not from heterogeneous compilations like this work) and converted the published abundance quantities (typically  $[\text{X}/\text{H}]$  or  $[\text{X}/\text{Fe}]$ ) to  $\log_{\epsilon}(\text{X})$  values using the solar abundance scale quoted in each paper. The complete sample of metal-poor stars used in this work, along with their stellar parameters and the references to the original literature are listed in Table 1.

In several cases there were more than one set of chemical abundances quoted for a single star. In these scenarios we opted for the most 'representative' chemical abundances. Specifically we opted for chemical abundances measured using (3D) model photospheres, abundances adjusted using trustworthy non-local thermodynamic equilibrium (LTE)

corrections, or abundances measured from ionised species (over neutral species) wherever possible. These choices were adopted to minimise systematic effects (e.g., non-LTE departures), which can be significant in EMP stars.

Our literature search revealed many low-metallicity stars with abundance measurements for just a few elements. These stars were faint (some with  $V \sim 20$ ), and therefore require a significant 8 m-class telescope time investment merely to confirm their metal-poor nature. Low S/N and/or limited wavelength coverage further precluded any detailed chemical analysis of these stars. This point highlights the need for apparently bright EMP stars, where the detailed chemistry can be inferred using existing telescope/instrument combinations (e.g., Schlafman & Casey 2014; Casey & Schlafman 2015). Previous studies (e.g., Bessell et al. 2015) have commented on the necessity of C, N, and other light-element abundances in order to accurately infer supernova progenitor masses. For these reasons, literature stars with just a few (typical  $\alpha$ -capture) elemental abundances were excluded from this work, as they cannot sufficiently constrain supernova models. We further excluded stars where there was ambiguity in the stellar parameters (and therefore the chemistry), usually where a star is equally likely to be a dwarf or sub-giant.

## 3 MASS AND IMF FITTING

With the assembled chemical abundances for all metal-poor stars, we used the **STARFIT**<sup>2</sup> code to infer progenitor masses, remnant masses and explosion energies. We used both the supernova models of Heger & Woosley (2010) and the Pair Instability models of Heger & Woosley (2002), and excluded Li abundances as they vary substantially throughout a star's lifetime. Similarly, due to CNO cycling, we opted to fit the sum of C, N, and O abundances simultaneously wherever possible rather than the individual abundances. As recommended by Heger & Woosley (2010), Sc and Cu were treated as model lower limits because they have multiple different nucleosynthetic pathways. We opted to exclude elemental abundances past the iron-peak ( $Z > 30$ ) as the nucleosynthetic origin of these elements in Population III stars is quite uncertain. Each **STARFIT** fit provides an explosion energy, a progenitor mass, a remnant mass, strength of mixing during the SN explosion, and a best-fit residual.

To quantify the uncertainty in derived progenitor masses, we perturbed the measured abundances for each star using their quoted uncertainties and queried **STARFIT** using the perturbed abundances. We adopted a conservative uncertainty of 0.2 dex for abundances without reported uncertainties. Measurements were assumed to be normally-distributed, and upper limits were perturbed by drawing values from a uniform distribution between  $[\text{X}/\text{H}] \sim \mathcal{U}(-8, L)$ , where  $L$  is the published limit in  $[\text{X}/\text{H}]$  format. We chose to draw from truncated uniform distributions for upper limits as Placco et al. (2015) notes low N abundances ( $[\text{N}/\text{H}] < -6$ ) are consistently predicted by **STARFIT** when only upper limits on nitrogen are available. Draws in  $[\text{X}/\text{H}]$  were converted

<sup>1</sup> Described in Suda et al. (2008, 2011) and Yamada et al. (2013) and available at <http://saga.sci.hokudai.ac.jp/wiki/doku.php>. The data were retrieved on 2015 August 7.

<sup>2</sup> Described in Chan et al. in prep and available through <http://www.starfit.org>.

to  $\log_e(X)$  before running STARFIT. We repeated this perturbation procedure thirty times for each star. We find four of the stars (HE0048-6408, HE0313-3640, HE2233-4724, and SMSSJ005953) to have extremely large ( $> 25$ ) best-fit residuals for all perturbations, and for this reason we discarded these stars from our sample. Numerical noise, uncertain physics (Sukhbold & Woosley 2014), and specifically the grid-like sampling of progenitor masses in supernova models implies that there is a systematic uncertainty floor for a given mass. Our tests demonstrated that a 10 per cent uncertainty in progenitor masses was sufficient to account for this sampling, which we take as representative of the error on the fit. We account for the distribution of recovered progenitor masses by means of a Monte Carlo technique when fitting the IMF. The distribution of inferred progenitor masses for each star, after fitting our perturbed abundance values are shown in Fig. 1

Sixteen of the stars in our sample also have SN progenitor mass estimates from Placco et al. (2015). Placco et al. use the same STARFIT tool as this work, yet report slightly different progenitor masses than what we find. There are several reasons for these discrepancies. Placco et al. adjust the C abundances based on the evolutionary state of the star, following empirical corrections derived in Placco et al. (2014). If no N measurement is available, the authors also assume  $[C/N] = 0$ . In contrast, we opt to fit the combined abundance of C, N, and O. This option is readily available in STARFIT, and implicitly accounts for CNO cycling and the evolutionary state of the star. Differences in abundance choices also contributed to discrepancies in progenitor masses. We employed lower model limits for Cu and Sc (the default recommended option), whereas Placco et al. quote model limits for Cr and Sc. Furthermore, for SMSS J031300.36-670839.3, we opted for the recommended abundances by Bessell et al. (2015), whereas Placco et al. employed the 1D LTE abundances. It also appears that some abundances for elements with  $Z < 30$  are not included in the Placco et al. fits. For example, the first star in Fig. 8 of Placco et al., SDSS J220924.70-002859.0, is missing both the Na measurement and O upper limit from Spite et al. (2013).

The combination of these discrepancies and analysis choices explains all differences in the inferred progenitor masses; by replicating the Placco et al. *StarFit* options, adjusting C and assuming  $[C/N] = 0$ , and excluding abundances not present in their Figure 8, we were able to reproduce all of their inferred progenitor masses. It is reassuring to see that even with the systematic differences that arise from using different STARFIT settings, the difference in inferred progenitor masses are reasonably encapsulated by our total uncertainties.

We examined the distribution of derived masses from STARFIT as a function of  $T_{\text{eff}}$ ,  $\log g$ , and  $[\text{Fe}/\text{H}]$ . There is no obvious trend of progenitor mass with stellar parameters, which suggests that our data are not introducing a systematic bias. Encouragingly, we see that of the three stars in our sample with precursor SN masses of  $> 70 M_{\odot}$ , there is a spread in  $[\text{Fe}/\text{H}]$  between  $-5.0$  and  $-3.6$  dex.

The Initial Mass Function can be defined as  $\xi(M) = AM^{-\alpha}$  where  $\xi(M)$  is the probability of finding a star of mass  $M$ , the exponent  $\alpha$  is the “slope” of the IMF, and  $A$  is a normalisation constant (Salpeter 1955). To de-

termine the number of stars between masses  $M_1$  and  $M_2$ , we simply integrate with respect to  $M$ , over the range  $M_1$  to  $M_2$ . When fitting the observed distribution of Population III supernova progenitor masses to the IMF, we have three free parameters:  $\alpha$ , and the minimum and maximum mass for a SN progenitor,  $M_{\text{min}}$  and  $M_{\text{max}}$  respectively. As can be seen from Fig. 1, the masses derived for each progenitor when perturbing abundances are not normally distributed. We hence employed a Monte Carlo technique, where we fit the IMF to our observed data 50,000 times. For each iteration, we randomly draw a mass for each star from the 30 perturbed measurements, discarding any masses where STARFIT returned a residual of greater than 3 when fitting abundances. The parameters of the IMF from each Monte Carlo iteration were simply taken as those values which minimised the  $\chi^2$  value of the fit, as shown in Fig. 2. The constraint that the residual of the STARFIT model must be  $< 3$  reduces the size of the sample from 49 stars to 29.

Given the progenitor masses in shown in Fig. 1, the best fit values (and 16th/84th percentile uncertainties) we infer for the IMF are  $\alpha = 2.35^{+0.29}_{-0.24}$ , a formal minimum SN progenitor mass of  $M_{\text{min}} = 8.5^{+0.2}_{-0.4} M_{\odot}$  and a maximum SN progenitor mass of  $M_{\text{max}} = 87^{+13}_{-33} M_{\odot}$ . Since the minimum mass for Population III supernovae in the data base is  $9.6 M_{\odot}$ , however, the conclusion is that the lower IMF endpoint must lie below the minimum mass for Population III supernovae. From the present data, no conclusion can be drawn, however, how far below that may be.

## 4 DISCUSSION AND CONCLUSIONS

Overall, the fit to the inferred Population III supernova progenitor masses found in Sect. 3 appears quite good. In detail, there are three mass ranges where the quality of the fit appears to vary. Above  $30 M_{\odot}$  the inferred masses match the fitted IMF extremely well. We find that the distribution of possible maximum masses for a Population III supernova progenitor to be roughly bimodal, with a main peak at  $\sim 90 M_{\odot}$ , and a smaller peak at  $\sim 50 M_{\odot}$ . There is a small tail of Monte Carlo trials which accommodate an upper mass limit of  $\lesssim 120 M_{\odot}$ , but none above this. We also note that the upper mass limit is relatively insensitive to  $\alpha$ .

Between  $15 M_{\odot}$  and  $30 M_{\odot}$ , the inferred progenitor mass distribution appears to lie slightly below the best fit IMF. The models to which we fit the abundances have masses in steps of at most  $0.5 M_{\odot}$  over this mass range, so grid effects are unlikely to be the cause of this. An alternative possibility is that an appreciable fraction of stars with zero-age main sequence masses in the range  $15\text{--}30 M_{\odot}$  massive stars do not explode as SN but make black holes instead (Sukhbold & Woosley 2014), and hence do not eject their synthesised material to enrich subsequent generations of star formation.

Below  $15 M_{\odot}$  the inferred masses appear to follow a somewhat steeper IMF than our best fit, suggesting that the exponent  $\alpha$  may be slightly higher. The IMF is pulled towards shallower slopes (i.e., smaller values of  $\alpha$ ) by the stars in the  $15\text{--}30 M_{\odot}$  range. If these were excluded, then the fit could better accommodate the lower mass stars, although we are wary of arbitrarily removing stars to improve the fit. The formally deduced minimum mass of  $8.5^{+0.2}_{-0.4} M_{\odot}$

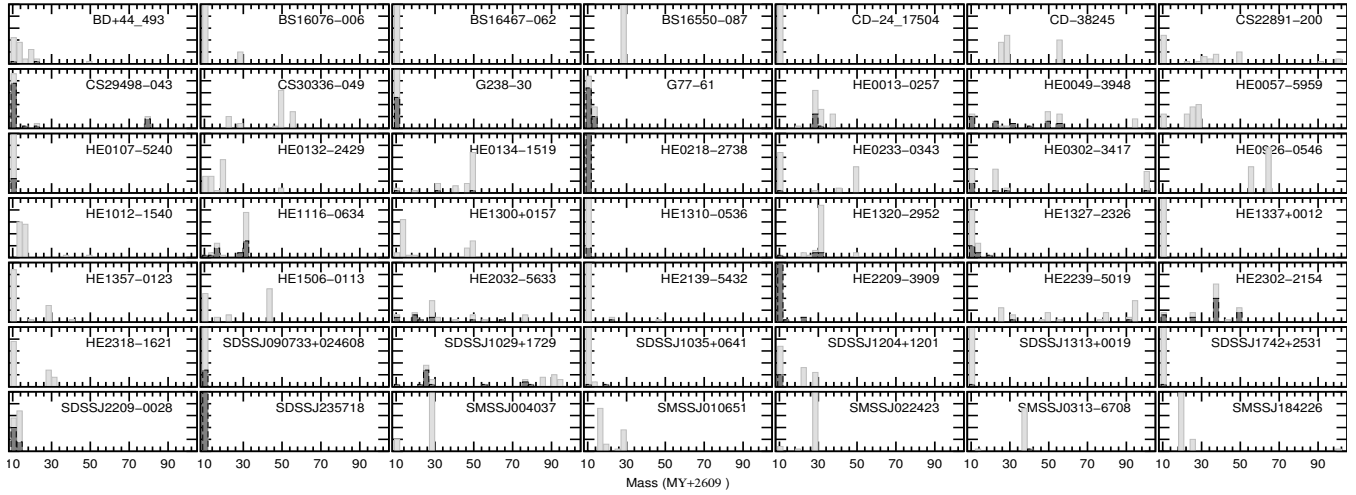


**Figure 1.** Histograms of derived masses from 30 iterations of STARFIT using perturbed abundances. Light grey bars show fits with a residual of  $<25$ , while black lines show fits with a residual of  $<3$ .

**Table 1.** Metal-poor star abundances used in this study. The full table is available online, a portion of it is shown here for guidance.

Star	$\alpha$ (J2000) [hms]	$\delta$ (J2000) [hms]	$T_{\text{eff}}$ (K)	$\log(g)$	[Fe/H]	$\xi$ [km s $^{-1}$ ]	Source
BD+44 493	02:26:49.7	+44:57:46	5430	3.4	-3.8	1.3	Ito et al. (2013)
BS 16076-006	12:48:22.7	+20:56:44	5199	3.0	-3.81	1.4	Bonifacio et al. (2009)
BS 16467-062	13:42:00.6	+17:48:40	5388	3.04	-3.7	1.7	Lai et al. (2008)

from statistical sampling lies well below the minimum mass for Population III supernovae as reflected by stars in the model data base. We can infer that there is no evidence that the minimum mass for a Population III SN was significantly higher than eight solar masses. However, as the lower mass limit is close to the edge of the model grid at  $10M_{\odot}$  we stress that we cannot determine from this data whether the IMF for all stars (and not just those that explode) extends to much lower masses.

As a test, we also relaxed our constraint that the residual of the STARFIT models must be  $<3$ , and allowed for models with a residual of up to 10. 46 stars had acceptably fitted masses, and these gave a lower limit of  $\sim 8.5 M_{\odot}$ , and an upper mass limit of between 70 and  $110 M_{\odot}$ . Again, a contribution from stars above  $125 M_{\odot}$  can be excluded at high significance, although interestingly the fit prefers a flatter IMF slope of  $\sim 1.9$ .

We find the best fit value of the exponent in the IMF to be 2.35, which is identical to the canonical value of Salpeter (1955), and perhaps suggests that star formation in the metal free Universe is not so dissimilar to that in the present day. We see no evidence for stars above  $\sim 120M_{\odot}$  exploding and no signs of the hypothesised pair-instability SNe which may have enriched the universe at the earliest times. We cannot exclude, however, that there are narrow windows where high mass ( $>200 M_{\odot}$ ) stars may explode.

We note that the fact that perturbing abundances within their quoted uncertainties affects the inferred progenitor mass to such a large extent (as shown in Fig. 1) demonstrates the necessity of propagation or sampling techniques to account for the full distribution of progenitor masses.

Finally, we emphasize that our abundance probe is only a reflection of the fraction of stars that do explode as SNe; we have no probe of stars that don't explode because they make black holes or are too low mass. Variation in explosion energy, the amount of matter that is enriched by supernovae of a given mass, and the potentially environment-dependent fraction of such gas forming low-mass stars, may also affect the conclusions drawn above and will require further extended studies of first star formation and death.

## ACKNOWLEDGMENTS

This work was supported by the European Union FP7 programme through ERC grant number 320360. AH was supported by Australian Research Council through a Future Fellowship (FT120100363). This research has made use of the SIMBAD database, operated at CDS, Strasbourg, France, the SAGA database (Suda et al. 2008), NASA's Astrophysics Data System, the excellent TRIANGLE package (Foreman-Mackey et al. 2014), and Astropy (Astropy Collaboration et al. 2013).

## REFERENCES

- Astropy Collaboration et al., 2013, *A&A*, 558, AA33
- Bastian N., Covey K.R., Meyer M.R., 2010, *ARAA*, 48, 339
- Beers T.C., Christlieb N., 2005, *ARAA*, 43, 531
- Bessell M.S. et al., 2015, *ApJL*, 806, L16
- Bromm V., Coppi P.S., Larson R.B., 1999, *ApJL*, 527, L5

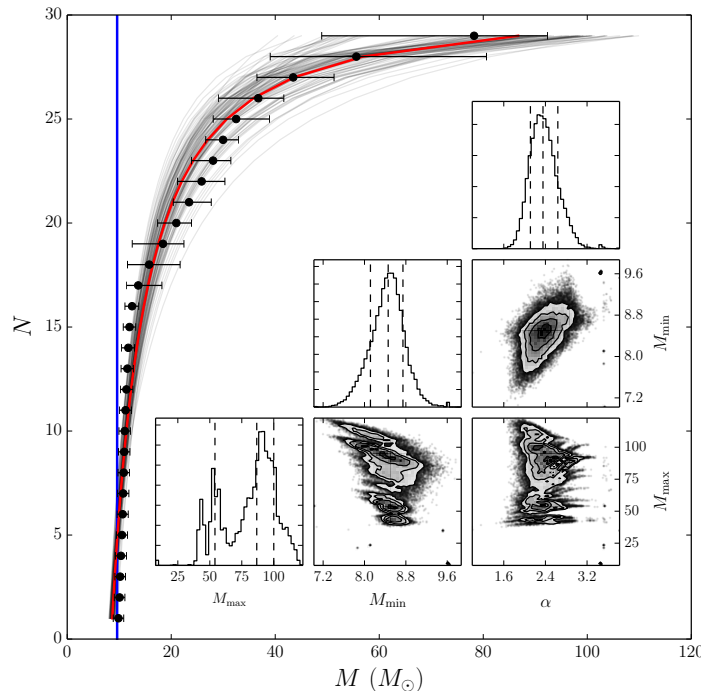


**Figure 2.** Main panel: The cumulative distribution of Population III supernova progenitor masses to which the IMF was fit. Black points show the mean mass of the  $n$ th star across all Monte-Carlo iterations. Error bars correspond to the 16th and 84th percentile ranges (i.e.,  $\simeq 1\sigma$  of the mass of the  $n$ th star, added in quadrature with the 10 percent error floor.) The light grey lines show 100 IMFs as fitted during Monte-Carlo iterations, while the red line shows the final best fit IMF. The blue vertical line shows the lower mass limit of  $9.6 M_{\odot}$  for the model grid used with STARFIT. Inset panel: Best fit values for  $\alpha$ ,  $M_{\min}$  and  $M_{\max}$  from 50,000 Monte-Carlo iterations. The distribution of values for each parameter is shown with a histogram, and the best fit value and 16th and 84th percentile limits are marked with dashed lines.

Bonifacio P. et al., 2009, A&A, 501, 519

Casey A.R., Schlafman K.C., 2015, ApJ, 809, 110

Chen K.-J., Bromm V., Heger A., Jeon M., Woosley S.E., 2015, ApJ, 802, 13

Christlieb N., Schörck T., Frebel A., Beers T.C., Wisotzki L., Reimers D., 2008, A&A, 484, 721

Clark P.C., Glover S.C.O., Smith R.J., Greif T.H., Klessen R.S., Bromm V., 2011, Science, 331, 1040

Foreman-Mackey, D., Price-Whelan, A., Ryan, G., et al. 2014, Zenodo, 10.5281/zenodo.11020

Greif T.H., Springel V., White S.D.M., Glover S.C.O., Clark P.C., Smith R.J., Klessen R.S., Bromm V., 2011, ApJ, 737, 75

Heger A., Woosley S.E., 2002, ApJ, 567, 532

Heger A., Fryer C.L., Woosley S.E., Langer N., Hartmann D.H., 2003, ApJ, 591, 288

Heger A., Woosley S.E., 2010, ApJ, 724, 341

Ito H., Aoki W., Beers T.C., Tominaga N., Honda S., Carollo D., 2013, ApJ, 773, 33

Jacobson H.R. et al. 2015, ApJ, 807, 171

Ji A.P., Frebel A., Bromm V., 2015, arXiv:1508.06137

Lai D.K., Bolte M., Johnson J.A., Lucatello S., Heger A., Woosley S.E., 2008, ApJ, 681, 1524

Norris J. E. et al. 2013, ApJ, 762, 25

O'Shea B.W., McKee C.F., Heger A., Abel T., 2008, First Stars III, 990, 13

Placco V.M., Frebel A., Beers T.C., Christlieb N., Lee Y.S., Kennedy C.R., Rossi S., Santucci R.M., 2014, ApJ, 781,

40

Placco V.M., Frebel A., Lee Y.S., Jacobson H.R., Beers T.C., Pena J.M., Chan C., Heger A., 2015, ApJ, 809, 136

Salpeter E.E., 1955, ApJ, 121, 161

Schaerer D., 2002, A&A, 382, 28

Schlaufman K.C., Casey A.R. 2014, ApJ, 797, 13

Sobral, D., Matthee, J., Darvish, B., Schaerer D., Mobasher B., Röttgering H.J.A., Santos S., Hemmati S., 2015, ApJ, 808, 139

Sukhbold T., Woosley S.E., 2014, ApJ, 783, 10

Suda T. et al. 2008, PASJ, 60, 1159

Suda T., Yamada S., Katsuta Y., Komiya Y., Ishizuka C., Aoki W., Fujimoto M.Y., 2011, MNRAS, 412, 843

Sukhbold T., Woosley S.E., 2014, ApJ, 783, 10

Spite M., Caffau E., Bonifacio P., Spite F., Ludwig H.-G., Plez B., Christlieb N., 2013, A&A, 552, A107

Tominaga N., Iwamoto N., Nomoto K., 2014, ApJ, 785, 98

Whalen D.J., Fryer C.L., Holz D.E., Heger A., Woosley S.E., Stiavelli M., Even W., Frey L.H., 2013, ApJL, 762, L6

Fryer, Chris L.; Holz, Daniel E.;

Yamada S., Suda T., Komiya Y., Aoki W., Fujimoto M. Y.,

2013, MNRAS, 436, 1362